Journal of the Korean Astronomical Society
54: 113 ∼ 119, 2021 August

https://doi.org/10.5303/JKAS.2021.54.4.113
pISSN: 1225-4614 · eISSN: 2288-890X
http://jkas.kas.org

Tilt Correction for a Wide-field On-axis Telescope Using the Symmetricity of Optical Aberrations

Chung-Uk Lee[1], Yunjong Kim[1], Seung-Lee Kim[1], Dong-Joo Lee[1,2], Sang-Mok Cha[1,3], Yongseok Lee[1,3], and Dong-Jin Kim[1]

[1]Korea Astronomy and Space Science Institute, Daejeon 34055, Korea; leecu@kasi.re.kr
[2]Department of Astronomy and Space Science, Chungbuk National University, Cheongju 28644, Korea
[3]School of Space Research, Kyung Hee University, Yongin 17104, Korea

Received December 18, 2020; accepted June 21, 2021

Abstract: It is difficult for observers to conduct an optical alignment at an observatory without the assistance of an optical engineer if optomechanical parts are to be replaced at night. We present a practical tilt correction method to obtain the optimal optical alignment condition using the symmetricity of optical aberrations of a wide-field on-axis telescope at night. We conducted coarse tilt correction by visually examining the symmetry of two representative star shapes obtained at two guide chips facing each other, such as east–west or north–south pairs. After coarse correction, we observed four sets of small stamp images using four guide cameras located at each cardinal position by changing the focus positions in 10-μm increments and passing through the optimum focus position in the range of $\pm$200 μm. The standard deviation of each image, as a function of the focus position, was fitted with a second-order polynomial function to derive the optimal focus position at each cardinal edge. We derived the tilt angles from the slopes converted by the distance and the focus position difference between two paired guide chip combinations such as east–west and north–south. We used this method to collimate the on-axis wide-field telescope KMTNet in Chile after replacing two old focus actuators. The total optical alignment time was less than 30 min. Our method is practical and straightforward for maintaining the optical performance of wide-field telescopes such as KMTNet.

Key words: telescopes — instrumentation: miscellaneous — techniques: photometric — methods: observational

1. Introduction

The Korea Astronomy and Space Science Institute (KASI) installed three identical 1.6-meter telescopes in Chile, South Africa, and Australia to search for exoplanets with the microlensing method (Kim et al. 2016). Each telescope of this Korea Microlensing Telescope Network (KMTNet) is located at a similar latitude of around $-32°$, enabling uninterrupted 24-hour observations with a high cadence. Since the commissioning of KMTNet in 2015, many new types of light curves exhibiting rapid variability on time scales of less than 24 h have been observed and analyzed (Han et al. 2017, 2020; Hwang et al. 2018a,b; Udalski et al. 2018; Jung et al. 2019, 2020; Gould et al. 2020). KMTNet opened a new era of microlensing science by analyzing these short-time-scale anomalous features.

However, it is difficult to maintain the optical performance and good condition of the three telescopes, and this is closely related to the photometric performance and consistency of these systems. To maintain the three systems, engineers periodically visit the observatories, but a sudden need to replace optomechanical parts directly and immediately affects optical performance. We replaced two old actuators that were located at the east (#1 in Figure 1a) and west (#3 in Figure 1a) at the KMTNet-CTIO observatory during a regular maintenance visit in December 2019. After the actuators were replaced, the PSFs of the science images appeared severely deteriorated; thus, an x/y-tilt adjustment was required. These optical misalignment issues can cause the photometric uncertainty observed in the light curves (Kim et al. 2018) produced by the KMTNet data reduction pipeline using difference image analysis (Woźniak 2000). Hence, a practical and straightforward method to maintain optics in sufficiently collimated condition is essential for KMTNet operation.

Many researchers have developed various algorithms and methods using Zernike polynomials for the optical alignment of wide-field telescopes and state-of-the-art optical instruments. Additionally, practical collimation techniques using aberrations have been introduced and discussed by several researchers. Mcleod (1996) presented a useful method to collimate the Mt. Hopkins 1.2-m telescope using distorted stellar image shapes obtained at eight field edges. Wilson & Delabre (1997) investigated the decentering astigmatism effects of the European Southern Observatory (ESO) New Technology Telescope (NTT). They concluded that the effect is negligible under sufficient alignment conditions such as those in the active-system ESO NTT. However, the decentering astigmatism effects of a wide-field telescope are particularly critical at the edge field. Noethe

Corresponding author: C.-U. Lee

& Guisard (2000) derived analytical expressions for field astigmatism and applied them to the collimation of the ESO Very Large Telescope (VLT). Schechter & Levinson (2011) displayed third-order and fifth-order generic misalignment aberration patterns with illustrations.

The purpose of this study is to provide a practical and straightforward method to maintain optimal optical alignment conditions without employing a complicated numerical algorithm. We monitor four cardinal edge fields simultaneously and use the relationship between the tilt angle variation and aberration patterns, especially astigmatism, of the lens barrel of the KMTNet at the edge of the fields. We can remove misalignment-induced aberrations effectively when the optical aberration pattern is symmetric at the out-of-focus position. We use the similar concept of Mcleod (1996) for coarse collimation using visual examination, but the tilt angles are quantitatively derived from slopes converted by the distance and focus position difference between two paired guide charge-coupled device (CCD) chip combinations, such as east–west and north–south. In this study, we conduct tilt correction at the KMTNet-Cerro Tololo Inter-American Observatory (CTIO).

2. FOCUS MONITORING USING GUIDE CAMERA

2.1. KMTNet Focusing System

Modern telescope systems contain an auto-focusing function that keeps the spot size as small as possible during observations. Observers typically attempt to optimize the focus condition in the entire focal plane during nighttime observations. However, it is difficult to judge the optimum focus state during observation. Particularly, the adjustment effect can be negligible under poor weather conditions.

Most optical telescopes for wide field survey adopt the prime focus design, which consists of two optical components: a mirror and a prime focus assembly (PFA). The focusing system of the KMTNet telescope is designed to allow simultaneous x/y-tilt and focus adjustments using three actuators installed on the top ring of the telescope (Poteet et al. 2012). We adapted the patented Harmonic Drive actuator model that minimizes mechanical backlash to achieve a minimum repeatable resolving accuracy of 1 μm. The actuators are located at each vertex of an equilateral triangle on the top ring which has a diameter of 2017.6 mm, as illustrated in Figure 1a. Actuator #2 is installed at due south, and the other two actuators (#1 and #3 to the east and west, respectively) are placed north of the optical center. The distance between the optical axis and actuator #2 is 1008.8 mm, the distance between actuators #1 and #3 is 1747.3 mm, and the distance between actuator #2 and the midpoint between actuators #1 and #3 is 1513.2 mm.

The focal plane of the KMTNet CCD camera is occupied by four e2v CCD290-99 chips with dimensions of 10 μm × 9,216 pixels × 9,232 pixels for science imaging (Figure 1b). Additional four e2v CCD47-20 chips measuring 13 μm × 1024 pixels × 1024 pixels were installed

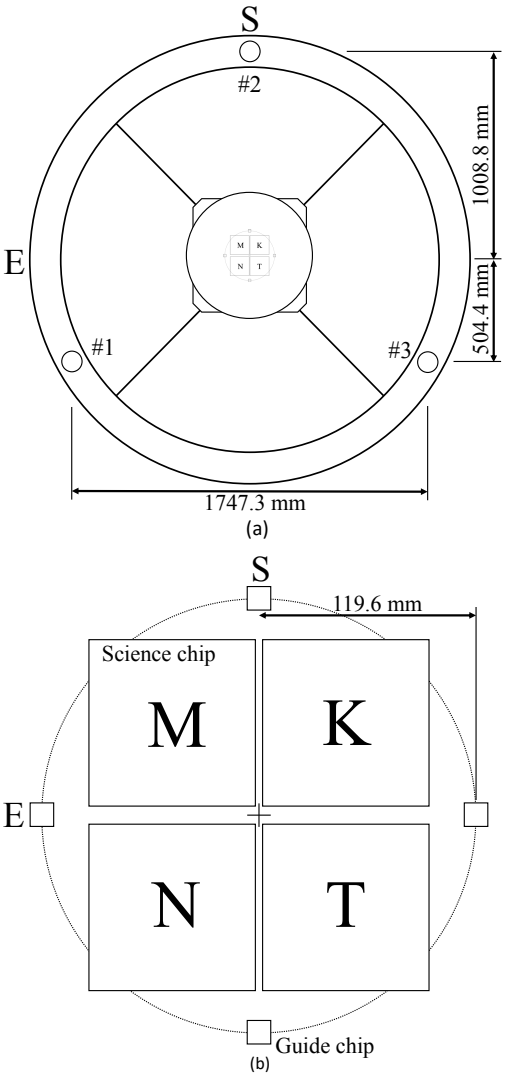

Figure 1. (a) Positions of the three actuators installed on the top ring. The numbers in the figure represent the positions of three actuators. A specially designed holding fixture is installed on the tapped hole of each actuator. (b) Focal plane layout. Four large squares indicate science CCD chips, and small rectangles at the four cardinal directions represent guide CCD chips.

to guide the telescope. The guide chips are placed toward the four cardinal directions and 119.6 mm away from the focal plane optical center, where misalignment aberrations such as coma and astigmatism are increased. The locations of and distances between the actuators and guide CCDs are not the same in the x-y coordinate system; thus, a conversion ratio is used for x/y-tilt adjustment according to the east–west and north–south directions. Actuators #1 and #3 are adjusted by the same amount of displacement in opposite directions to correct the x-tilt angle (east–west direction). For the y-tilt angle (north–south direction), actuator #2 is adjusted in the opposite direction of actuators #1 and #3 at a 1:2 displacement ratio. Focus adjustment is performed by moving the three actuators

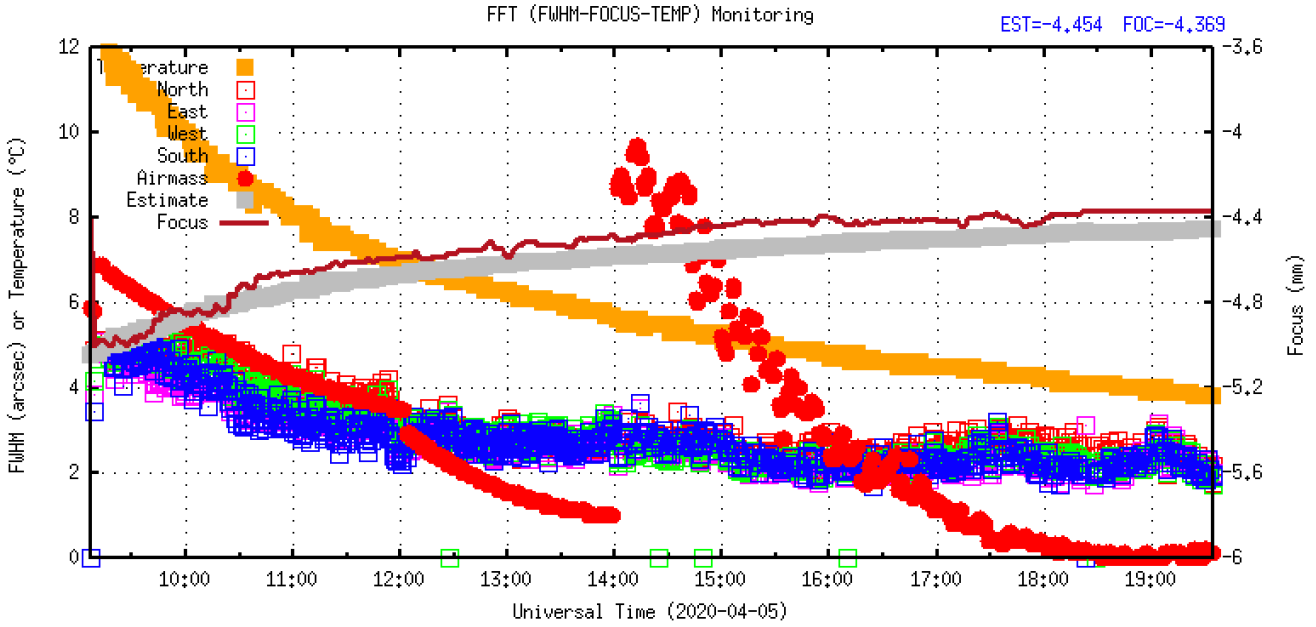

Figure 2. Sample guide monitoring plot, showing variations in FWHM, focus, and temperature with time. Each FWHM measurement in the four cardinal positions is indicated by open squares of different color. Gold-filled squares represent relative temperature variation. Silver-filled squares represent estimated focus position based on the thermal expansion of the telescope structure. The brown line represents actual focus positions read from the actuators. Red-filled circles indicate $\sec Z$ of the observation target. The GMON program contains an auto-correction function. However, observers attempted to find optimal focus by manually adjusting the focus position. The disagreement between the silver squares and the brown line exhibits this effort.

in the same direction simultaneously.

2.2. Software for Focus and Tilt

We developed two graphical user interface (GUI) programs to achieve this function by controlling four guide cameras and three focus actuators: a guide monitoring (GMON) interface and a tilt controlling (TCON) interface. GMON takes images and provides focus information via two panels that display the PSFs of the four cardinal directions and a plot of the FWHM variations over time, and TCON controls three actuators using GUI buttons.

The GMON program obtains a representative point spread function (PSF) from guide CCD images and provides a focus correction value, which is, essentially, calculated from the thermal expansion of the telescope steel structure. Observers typically run the GMON program when observation begins. Then, two graphic panels are displayed on a monitor screen: the representative PSF shapes on the guide CCDs obtained at four cardinal directions and the measured full-width-at-half-maximum (FWHM) variation with time. When the shutter is open, GMON takes guide images with a 10-second exposure and automatically saves them. The saved images are then processed using Source Extractor (Bertin & Arnouts 1996) and PSF Extractor (Bertin 2011) to extract the representative PSFs of the four cardinal positions. Contour lines are then overlaid onto the PSF images to make it easier to judge the distorted shape. Figure 2 displays a screenshot of GMON measurements. The estimated focus value calculated from the structure temperature is represented by silver squares, while the actual focus value measured from the actuator encoders is represented by a brown line. Minor disagreements between estimation and measurement reflect the observer's effort to find the best focus during observation.

The TCON program interactively controls the three actuators for x/y-tilt correction of the wide-field corrector barrel to the mirror. The observer visually checks whether the four representative PSFs are symmetrical and adjusts the x/y-tilt angle using the GUI buttons in the TCON program. TCON is helpful to control the x/y-tilt angle of the PFA, which is composed of field correcting lenses and a CCD camera.

3. Sensitivity Analysis of KMTNet Optical System

3.1. KMTNet Optical System

The KMTNet telescope optical design uses a parabolic surface for the 1.6-m mirror and spherical surfaces for all four corrector lenses. These surfaces are polished with high precision in optical shops without any significant technical challenges. The error budget of the optical alignment of KMTNet was carefully considered not to be too tight, even though it is a wide-field telescope with a $2^\circ \times 2^\circ$ field of view. According to the final optical design, the most sensitive optical component of the field corrector lens group is lens #2, which exhibits a diameter of 416 mm and a decentering assembly tol-

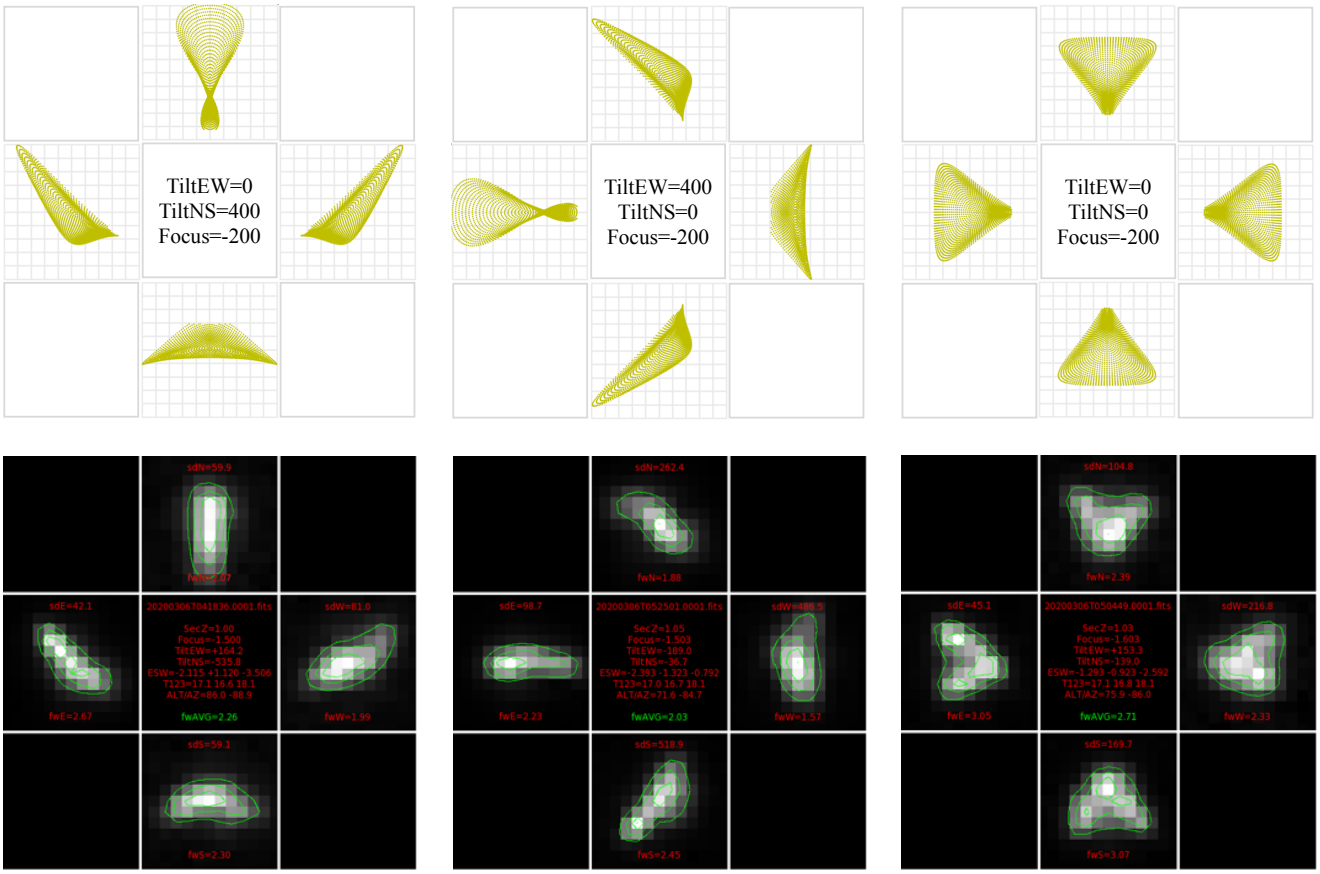

Figure 3. Simulated `Zemax` spot diagrams (top panels) and observed PSF images at four guide camera locations (bottom panels). *Left panels:* For a y-tilt (north–south) angle of 400″ and a focus error of 200 μm. *Center panels:* For a x-tilt (east–west) angle of 400″ and a focus error of 200 μm. *Right panels:* For a focus error of 200 μm and no tilt error.

erance of 50 μm. Each lens was accurately placed with a tolerance of 3 μm and potted with an RTV560 bond in the lens cell using a precision turntable in the optical shop.

The assembled corrector lens barrel was tested and certified using an auto-collimation test and a Hindle sphere. Because the wide-field correcting optics and direct imaging camera are assembled in one massive barrel structure, alignment of KMTNet is simplified to the collimation of two optical components. From the system alignment sensitivity analysis, we know that the relative decentering tolerance of the 1.6-m mirror to the corrector lens barrel is 90 μm. An optical alignment process based on star testing was conducted during the installation phase. The final optical alignment of the system was confirmed using a specially designed computer-generated hologram plate and interferometer, as illustrated by Oh et al. (2014).

3.2. Sensitivity Analysis

A `Zemax` simulation of the KMTNet optical design demonstrates that astigmatism is more significant than coma by a factor of six when there is a tilt error in the optical alignment. The linear-field astigmatism is a dominant factor in KMTNet, similar to other classical on-axis wide-field optical telescopes (Wilson & Delabre 1997; Noethe & Guisard 2000). Schechter & Levinson (2011) demonstrated the astigmatic field pattern when the optical alignment entails a tilt or decentering error. Therefore, the tilt error can be identified from the spot shape at the edge of the field, where the four guide CCDs are located, if it contains astigmatism.

From the `Zemax` analysis, we found that the misalignment aberration features are clearly visible at the four guide cameras when the focus is 200 μm away from the optimum position. We modeled a y-tilt (north–south direction) error of 400″ to observe the change of the asymmetric astigmatic aberration pattern. Figure 3 presents a comparison of the observed PSF shapes and the `Zemax` models at four guide chip positions having a misalignment error in x/y-tilt (primarily astigmatism), which shows a good agreement. A defocus of 200 μm toward the 1.6-m mirror was introduced to magnify the aberration features. KMTNet is an on-axis optical system; therefore the PSF shapes at the four guide chip cameras are symmetric in both the north–south and east–west directions when no tilt angle is applied. In contrast, the PSF shapes exhibit a north–south asymmetry when a non-zero y-tilt angle is introduced, and an east–west asymmetry for a non-zero x-tilt angle.

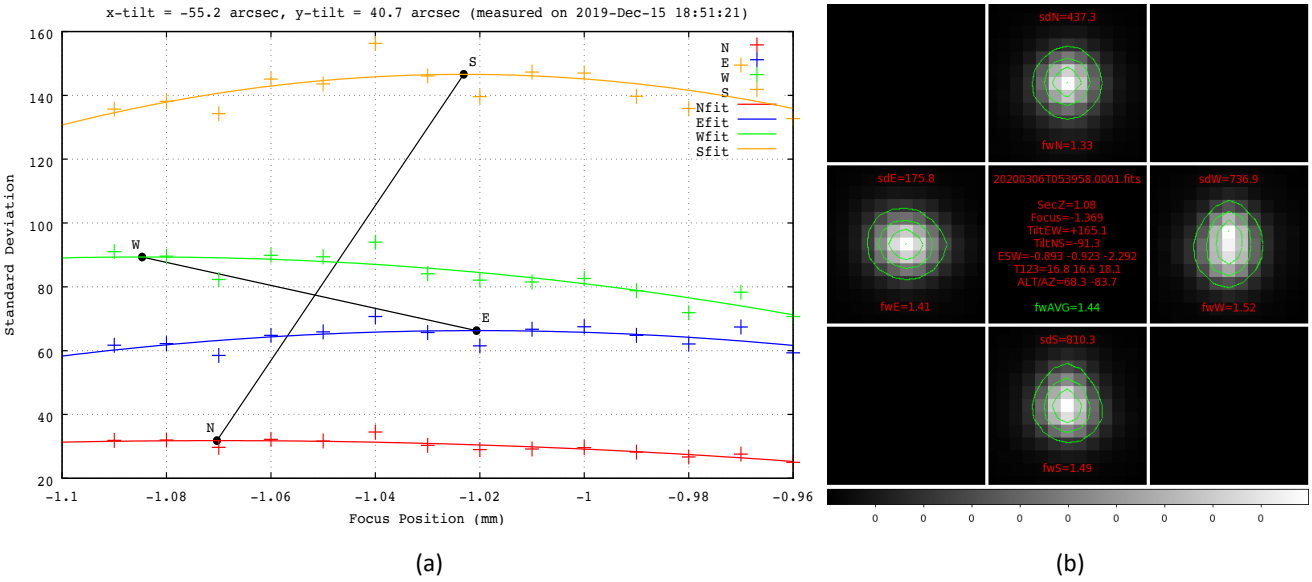

Figure 4. (a) Sample plot of a derivation of the final x/y-tilt angle, showing the standard deviation of the observed stamp image as a function of focus position. Each cardinal position optimal focus position, corresponding to maximum standard deviation, is marked with the corresponding letter. x/y-tilt angles are displayed at the plot top. (b) Representative PSF shapes at four cardinal directions after x/y-tilt correction.

4. TILT CORRECTION EXPERIMENT

4.1. Optimal Focus Position

The bottom panels of Figure 3 display variations of the PSF pattern as function of x/y-tilt. The tilt correction using the TCON program is intuitive, and a coarse optical alignment is easily achieved within a few minutes. After the coarse visual x/y-tilt adjustment, another script is executed to determine the best focus position and final x/y-tilt angle. The script controls the three actuators simultaneously, thereby varying the focus position from -200 μm to $+200$ μm at 10-μm increments, which includes the optimal focus position, and obtains four guide images at each focus position.

To derive the optimal focus position at each cardinal position, we conducted a test using two measurements: of the standard deviation of each stamp image and of the representative FWHM. We checked the correlation between the focus position and the representative FWHM of the stamp image at first. However, the correlation between focus position and the standard deviation of each stamp image was more straightforward for our purpose. Therefore, we concluded that the standard deviation of each stamp image as a function of the focus position is the more appropriate measurement to find the best focus.

4.2. Calculation of Tilt Angle

When the best-focus finding script execution is complete, all images are processed to derive the standard deviation of each stamp image, which is plotted as a function of the focus position. The best focus position for each guide camera position is determined by fitting the measurements with a second-order polynomial function (Figure 4a). We obtain four optimal focus position values, one for each cardinal position. The final x/y-tilt angle is calculated from the focus position difference ($\Delta_{\rm EW}$, $\Delta_{\rm NS}$) and the base distances ($d_{\rm EW}$, $d_{\rm NS}$) between the guide chips in each east–west and north–south pair, respectively:

$$\text{x-tilt} = \arctan\left(\frac{\Delta_{\rm EW}}{d_{\rm EW}}\right) \times 3600 \text{ arcsec}, \quad (1)$$

$$\text{y-tilt} = \arctan\left(\frac{\Delta_{\rm NS}}{d_{\rm NS}}\right) \times 3600 \text{ arcsec}, \quad (2)$$

where $d_{\rm EW}$ and $d_{\rm NS}$ are both 239.2 mm for KMTNet, as shown in Figure 1b.

After obtaining the four best focus positions, Equations (1) and (2) were used to calculate the tilt angles: $-55.2''$ for the x-tilt (east–west) and $40.7''$ for the y-tilt (north–south). Fine tilt correction was performed based on these values, and the final PSF results with the optimal focuses in the cardinal directions were obtained, as illustrated in Figure 4b. The average FWHM of four guide chips was $1.44''$ in this correction.

4.3. Improvement in Photometry

We investigated two sample images to determine the photometric uncertainty that is caused by the optical alignment error. These images were reduced with the image subtraction process of the KMTNet data reduction pipeline implemented by Lee et al. (2010). Figure 5a displays the result for an image having an x/y-tilt error. There is a diagonal gradient feature from the lower left to the upper right corner. In contrast, there is no distinguishable gradient feature and fewer black and white residuals in Figure 5b, which was derived from the image obtained after x/y-tilt correction.

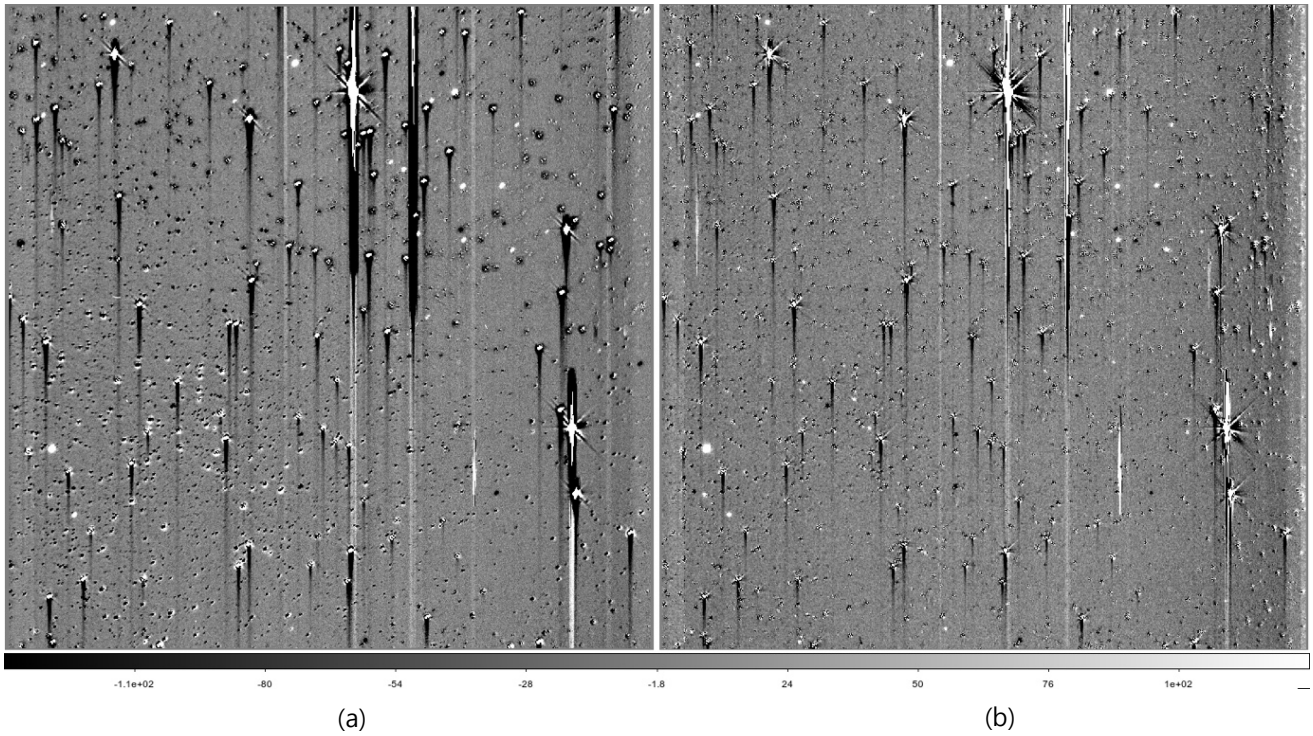

Figure 5. (a) Subtraction image before x/y-tilt correction. (b) Subtraction image after x/y-tilt correction. The vertical bleeding feature in the image is characteristic of the KMTNet CCD camera.

The black and white residual features surrounding stars produce an additional photometric uncertainty. Hence, It is evident that the x/y-tilt correction improves the photometric accuracy.

4.4. General Procedure to Find Tilt Angle

The KMTNet telescopes use three actuators to adjust the PFA, while most telescopes use only one actuator to adjust the focus. We generalize and refine the optical alignment procedure such that researchers can use this method in prime focus type wide-field telescopes with mechanical designs that differ from the one of KMTNet.

1. Match the east–west and north–south axes of the mirror adjustment bolts to the outermost edges of the CCD camera to measure the tilt angle.
2. Point the telescope to a crowded field, such as a cluster, so that an observer can observe stars on the four outermost edges of the CCD camera.
3. Adjust the focus position value within a range, which includes the optimal focus position, using a minimum focus adjustment step interval and observe at least 100 different focus position images.
4. Cut the image, beginning from its outermost edge, to a size of 128×128 pixels and calculate the standard deviation of each stamp image.
5. In each of the four data sets, find the focus position value corresponding to the maximum of the standard deviation.
6. Determine the focus position difference ($\Delta_{\rm EW}$, $\Delta_{\rm NS}$) and base distances of the outermost edge fields on the CCD ($d_{\rm EW}$, $d_{\rm NS}$) for the east–west and the north–south pairs, respectively.
7. Determine the x/y-tilt angles using Equations (1) and (2) and correct angles using the mirror tilt adjusting pivots located on the mirror cell.

5. SUMMARY

We present a practical and straightforward method for correcting the x/y-tilt error of a KMTNet telescope based on the symmetricity of optical aberrations at four cardinal edge fields without employing a complicated numerical algorithm. This method is sufficiently simple to be used for enhancing the photometric accuracy by immediately performing an optical alignment at the observatory during nighttime observations.

We developed and used two programs in this study: GMON, which conducts data acquisition, analysis, and visualization automatically; and TCON, which controls three actuators and adjusts the x/y-tilt angle of the telescope. The x/y-tilt error of the KMTNet-CTIO telescope was corrected in less than 30 minutes using this method. Using the proposed method, we obtained good-quality subtraction images that are essential for high-precision photometry.

We conducted x/y-tilt correction when the telescope was pointing to the zenith. In addition, further observations and automatic correction routines at low altitudes are required to compensate for the deformation of the optical alignment caused by changes in the

direction of gravity. An x/y-tilt compensation look-up table for each azimuth and altitude combination can be useful for making real-time corrections practical. A machine learning technique can be developed to maintain the optical alignment condition in real time.

We anticipate that this optical alignment method can collimate any wide-field on-axis telescope with a large format CCD camera. For general application in the field, certain small regions of interest of the four vertex edges of the rectangular CCD chip can adequately replace the four guide chips in the KMTNet telescope. Furthermore, this method is beneficial for field engineering purposes during night observation periods.

We also note that out study, although generalized to some extent, is heavily dependent on the KMTNet telescoped being equatorial-mount telescopes. Many telescopes have adopted the alt-azimuth mounts, which adds an image rotation mechanism to correct the field of view, thus increasing the degrees of freedom to be corrected. In addition, since the axis of the telescope changes with respect to the optical axis, the focus adjustment method for the secondary mirror support mechanism with a structure similar to the present one needs to be modified.

Acknowledgments

This research used the KMTNet system operated by KASI, and the data were obtained at the host site of CTIO in Chile. We are grateful for comments from anonymous reviewers and the editor of this journal.

References

Bertin, E., & Arnouts, S. 1996, SExtractor: Software for Source Extraction, A&AS, 117, 393

Bertin, E. 2011, Automated Morphometry with SExtractor and PSFEx, in: Evans, I. N., et al. (eds.), ASP Conf. Ser., 442, 435

Gould, A., Ryu, Y.-H., Calchi Novati, S., et al. 2020, KMT-2018-BLG-0029Lb: A Very Low Mass-Ratio Spitzer Microlens Planet, JKAS, 53, 9

Han, C., Udalski, A., Gould, A., et al. 2017, OGLE-2016-BLG-0613LABb: A Microlensing Planet in a Binary System, AJ, 154, 223

Han, C., Kim, D., Jung, Y., et al. 2020, One Planet or Two Planets? The Ultra-sensitive Extreme-magnification Microlensing Event KMT-2019-BLG-1953, AJ, 160, 17

Hwang, K.-H., Udalski, A., Ryu, Y.-H., Shvartzvald, Y., et al. 2018a, OGLE-2017-BLG-0173Lb: Low-mass-ratio Planet in a "Hollywood" Microlensing Event, AJ, 155, 20

Hwang, K.-H., Udalski, A., Bond, I. A., et al. 2018b, OGLE-2015-BLG-1459L: The Challenges of Exo-moon Microlensing, AJ, 155, 259

Jung, Y., Gould, A., Udalski, A., et al. 2019, Spitzer Parallax of OGLE-2018-BLG-0596: A Low-mass-ratio Planet around an M Dwarf, AJ, 158, 28

Jung, Y., Gould, A., Udalski, A., et al. 2020, OGLE-2018-BLG-1269Lb: A Jovian Planet with a Bright $I = 16$ Host, AJ, 160, 148

Kim, S.-L., Lee, C.-U., Park, B.-G., et al. 2016, KMTNet: A Network of 1.6 m Wide-Field Optical Telescopes Installed at Three Southern Observatories, JKAS, 49, 37

Kim, D.-J., Kim, H.-W., Albrow, M. D., et al. 2018, Korea Microlensing Telescope Network Microlensing Events from 2015: Event-finding Algorithm, Vetting, and Photometry, AJ, 155, 76

Lee, C.-U., Koo, J.-R., Kim, S.-L., et al. 2010, Detection of Variable Stars in the Open Cluster M11 Using Difference Image Analysis Pipeline, JASS, 27, 289

McLeod, B. A. 1996, Collimation of Fast Wide-Field Telescopes, PASP, 108, 217

Noethe, L., & Guisard, S. 2000, Analytical Expressions for Field Astigmatism in Decentered Two Mirror Telescopes and Application to the Collimation of the ESO VLT, A&AS, 144, 157

Oh, C. J., Frater, E., Lowman, A. E., et al. 2014, Development of a Wide Field Spherical Aberration Corrector for the Hobby Eberly Telescope: Design, Fabrication and Alignment, Proc. SPIE, 9145, 1

Poteet, W. M., Cauthen, H. K., Kappler, N., et al. 2012, Design and Fabrication of Three 1.6-meter Telescopes for the Korea Microlensing Telescope Network (KMTNet), Proc. SPIE, 8444, 1

Schechter, P.L., & Levinson, R. S. 2011, Generic Misalignment Aberration Patterns in Wide-Field Telescopes, PASP, 123, 812

Udalski, A., Ryu, Y.-H., Sajadian, S., et al. 2018, OGLE-2017-BLG-1434Lb: Eighth $q < 1 \times 10^{-4}$ Mass-Ratio Microlens Planet Confirms Turnover in Planet Mass-Ratio Function, AcA, 68, 1

Woźniak, P. R. 2000, Difference Image Analysis of the OGLE-II Bulge Data. I. The Method, AcA, 50, 421

Wilson, R. N., & Delabre, B. 1997, Concerning the Alignment of Modern Telescopes: Theory, Practice, and Tolerances Illustrated by the ESO NTT, PASP, 109, 53